

(E)-4-Aryl-4-oxo-2-butenoic Acid Phenylamides. Design, Antiproliferative Activity, Alignment Independent 3D QSAR Study Based on AMANDA Algorithm and Similarity on NCI-DTP Mechanistic Set

Maja D. Vitorović-Todorović, Aleksandra Erić*, Zorica Juranić*, Ivan O. Juranić**, Branko J. Drakulić***

Military-Technical Institute, Ratka Resanovića 1, Belgrade, mvitod@chem.bg.ac.rs

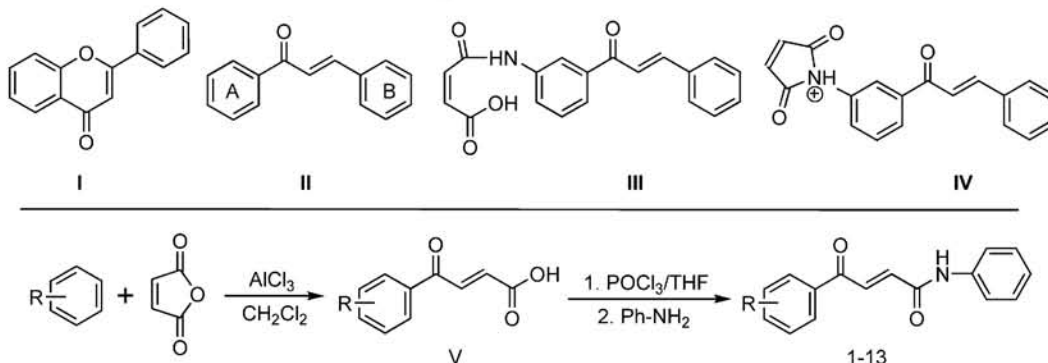
*Institute for Oncology and Radiology, Pasterova 14, Belgrade, Serbia

**Faculty of Chemistry, University of Belgrade, Studentski Trg 12-16, Belgrade, Serbia

***Department of Chemistry-IChTM, University of Belgrade, Njegoševa 12, Belgrade, Serbia

Introduction: Despite recent advances in understanding of biological processes involved in malignancies, there is persistent need for new and effective agents to bring the disease under control. Anticancer activity of natural products are continuously under investigation, because their good bioavailability and low toxicity. Flavonoids (**I**, Fig. 1), are prominent plant secondary metabolites, found in fruits, vegetables, olive oil and tea, consumed by humans as dietary constituents. A number of studies have demonstrated their anticancer activity.¹ Chalcones, 1,3-diaryl-2-propen-1-ones (**II**), are secondary metabolite precursors of flavonoids and isoflavonoids in plants; consisting of two aromatic rings joined by ketovinyl moiety, resemble open chain flavonoids. Diverse biological activities have been attributed to these compounds, including anticancer activity. Numerous SAR studies emerged.²⁻⁵ Biological activity of chalcones can be ascribed to their ability to act as Michael's acceptors with nucleophilic moieties, especially thiol groups of respective biological targets. It has been postulated that presence of 4-amino function on ring A of chalcone structure, protonated at physiological pH, increase their reactivity and thus antiproliferative activity.^{6,7} It has also been confirmed that *N*-alkylmaleimides exert antiproliferative activity by topoisomerase I inhibition.^{8,9} This led to design of 4-aminochalcone maleamic acids (**III**) and imides (**IV**).¹⁰ Most of these derivatives exert antiproliferative activity in low micromolar range. It has been shown that another type of molecules comprising ketovinyl moiety, *i.e.* aroylacrylic acids (**V**), exert antiproliferative activity toward HeLa cells,^{11a)} and other human dedifferentiated cell lines.^{11b)} Following this rationale, we design chalcone-aroylacrylic acid chimera, by incorporating amidic moiety between α,β -unsaturated carbonyl moiety and B phenyl ring of chalcone. Thus, we synthesized thirteen phenyl-substituted (E)-4-phenyl-4-oxo-2-butenoic acid phenylamides (**1-13**). In this communication, according to our best knowledge, for the first time antiproliferative activity of **1-13** toward two human tumor cell lines is reported.

Figure 1. Basic scaffolds (**I-IV**), as described in the text.



Scheme 1. Synthesis of **1-13**.

Methods: Synthetic pathway to **1-13** is given on Scheme 1. Friedel-Crafts acylation of commercially available substituted benzenes with maleic acid anhydride gives aroylacrylic acids (**V**).¹¹ **V** were converted to acid chlorides in dry THF by phosphorousoxichloride, then *in situ* reacted with equimolar amounts of aniline to give corresponding anilides in good yields¹². Obtained compounds were characterized by ¹H and ¹³C NMR and LC-HRMS (ESI). Antiproliferative potency of **1-13** toward FemX (human melanoma) and HeLa (human cervix carcinoma) cells were determined by MTT test.¹³ IC₅₀ Values (concentration of agent that induces 50% decrease in cell survival) are given in Table 1.

Modeling: Lowest energy conformers of **1-13** were obtained from SMILES by OMEGA,¹⁴ using MFF94s¹⁵ FF. Additional adjustment of geometry was done on PM6¹⁶ semiempirical level, by MOPAC2009,¹⁷ using VegaZZ¹⁸ as GUI and applying constraints on keto vinyl moiety. For alignment-free 3D QSAR analysis, molecules were submitted to Pentacle.¹⁹ Molecular interaction fields are computed using built-in GRID program,²⁰ and their filtration was done by AMANDA algorithm, as described in original reference.¹⁹ Five principal

components/latent variables were used for initial principal component analysis (PCA) and partial least square (PLS) model. Selection of variables was done by one/two cycle of factorial fractional design (FFD) for FemX/HeLa models, respectively. Validation of models was done by crossvalidation using three groups of approximately same size in which the objects are assigned randomly. Final models obtained by 2 latent variables (LV) were reported. Virtual screening on National Cancer Institute – Developmental Therapeutics Program (NCI-DTP) mechanistic database²¹ was also done by Pentacle VS mode, using 15 PC and AMANDA/MACC2 for discretization and encoding, respectively.

Results and Discussion: All examined compounds (**1-13**) exert antiproliferative activity in low micromolar to submicromolar concentrations (Table 1). FemX cells are more susceptible on action of compounds. The most potent against both cell lines are **8** and **6**, that bear *ortho*-alkyl substituents on aroyl phenyl ring. Alkyl-substituted compounds are more potent than halogen or alkoxy derivatives. The spatial arrangement of pharmacophoric points that contribute to potency against each examined cell line were examined by alignment-free 3D QSAR analysis. Molecular interaction fields obtained by GRID programme, using HBA (O), HBD (N1), hydrophobic (DRY) and shape (TIP) probes were used and GRID resolution of 0.4 Å. For filtration of nodes (discretization and encoding), AMANDA/CLAC algorithms were used. PLS coefficient plots obtained with 2 latent variables are shown on Figures 2 and 3, for HeLa and FemX cell lines, respectively. Statistics of PCA and PLS models are given in Tables 2 and 3, respectively.

Table 1. Compounds **1-13**, experimental and predicted IC₅₀'s toward HeLa and FemX cells.

Comp. N ^a	R-	Experimental IC ₅₀ (μM)		Predicted IC ₅₀ (μM)	
		HeLa	FemX	HeLa	FemX
1	H-	4.91 ± 0.99	2.20 ± 0.50	4.914	2.142
2	4- <i>i</i> -Pr-	3.09 ± 1.78	0.64 ± 0.13	2.820	0.684
3	4- <i>n</i> -Bu	1.06 ± 0.30	0.62 ± 0.06	1.098	0.603
4	4- <i>t</i> -Bu-	2.08 ± 0.35	0.69 ± 0.14	2.263	0.717
5	3,4-di-Me-	2.95 ± 0.27	1.84 ± 0.65	2.453	1.547
6	2,5-di-Me-	0.74 ± 0.13	0.62 ± 0.13	0.784	0.627
7	β-tetralinoyl-	2.11 ± 0.09	0.73 ± 0.16	2.411	0.816
8	2,4-di- <i>i</i> -Pr-	0.68 ± 0.13	0.59 ± 0.15	0.634	0.538
9	4-F-	2.99 ± 0.65	0.63 ± 0.32	3.417	/
10	4-Cl-	2.91 ± 0.29	2.84 ± 0.37	2.650	2.804
11	4-Br-	2.29 ± 0.98	2.30 ± 0.33	2.549	2.664
12	3,4-di-Cl-	2.80 ± 0.07	2.30 ± 0.28	2.698	2.268
13	4-OCH ₃ -	3.50 ± 0.54	2.34 ± 0.48	3.280	2.261

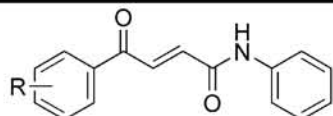


Table 2. PCA models

FemX					HeLa				
Comp.	SSX	SSX _{acc}	VarX	VarX _{acc}	Comp.	SSX	SSX _{acc}	VarX	VarX _{acc}
1	31.57	31.57	24.63	24.63	1	30.06	30.06	23.60	23.60
2	15.90	47.47	10.99	35.63	2	14.29	44.35	9.44	33.04
3	13.72	61.19	10.8	46.42	3	13.54	57.89	10.59	43.62
4	10.04	71.23	8.12	54.54	4	9.71	67.60	7.51	51.14
5	7.51	78.74	6.21	60.75	5	7.96	75.57	6.69	57.83

Comp. - Number of components; SSX - Percentage of the X sum of squares;
SSX_{acc} - Accumulative percentage of the X sum of squares; VarX - Percentage of the X variance;
VarX_{acc} - Accumulative percentage of the X variance.

640). Variable TIP-TIP 289 describes overall length of molecules; alkyl substituents on aroyl phenyl ring contributes to potency. Variable 336 emphasize importance of spatial arrangement between HBA and hydrophobic parts of molecules; again this is alkyl substituents on aroyl phenyl ring, including values of interaction energies of both HBD and hydrophobic probes. Variable N1-N1 183, expressed for potent **2** and **4**, and less potent **10-13**, describes interaction of HBD probe with both oxo functionalities of molecules, including respective interaction energies. Compound **9** is outlier, and we cannot offer explanation for this. For HeLa model, variables positively correlated with potency are DRY-N1 375 (expressed for **6**, **8** and **12**, Figure 5a) and N1-TIP 623 (absent for **3** and **4**, Figure 5b). The most interesting is 375, which emphasize importance of spatial arrangement between aroyl phenyl ring and aroyl oxo group for most active **6** and **8**. Short distance between DRY and N1 node (1.60 Å) could direct to interaction with one Tyr residue of respective biological target (so far just as speculation). Variable 623 describes spatial arrangement of amido NH group and substituents on aroyl phenyl ring. It should be noted that TIP node is located close to 2-*i*-Pr- substituent of **8**, and close to 5-Me-

For FemX model, variables positively correlated with potency – TIP-TIP 289 (Figure 4a), DRY-O 336 (Figure 4b) and O-TIP 640 (Figure 4c) are expressed for most potent **2-4**, **7** and **8** (and **6** for

Table 3. PLS models.

Comp.	FemX						
	SSX	SSX _a	SDEC	SDEP	R ²	R ² _{acc}	Q ² _{acc}
1	25.80	25.80	0.07	0.16	0.93	0.93	0.67
2	10.56	36.36	0.04	0.14	0.05	0.98	0.76
HeLa							
Comp.	SSX	SSX _a	SDEC	SDEP	R ²	R ² _{acc}	Q ² _{acc}
1	22.22	22.22	0.08	0.18	0.90	0.90	0.46
2	14.22	36.45	0.04	0.16	0.07	0.97	0.60

Comp. - Number of components; SSX - Percentage of the X sum of squares; SSX_{acc}- Accumulative percentage of the X sum of squares; SDEP- standard deviation error of the predictions.; R² - Coefficient of determination; R²_{acc} – Accumulative coefficient of determination; Q²_{acc} – Accumulative squared predictive correlation coefficient.

Figure 2. 2LV PLS coefficients plot for FemX model.

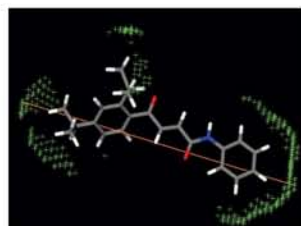
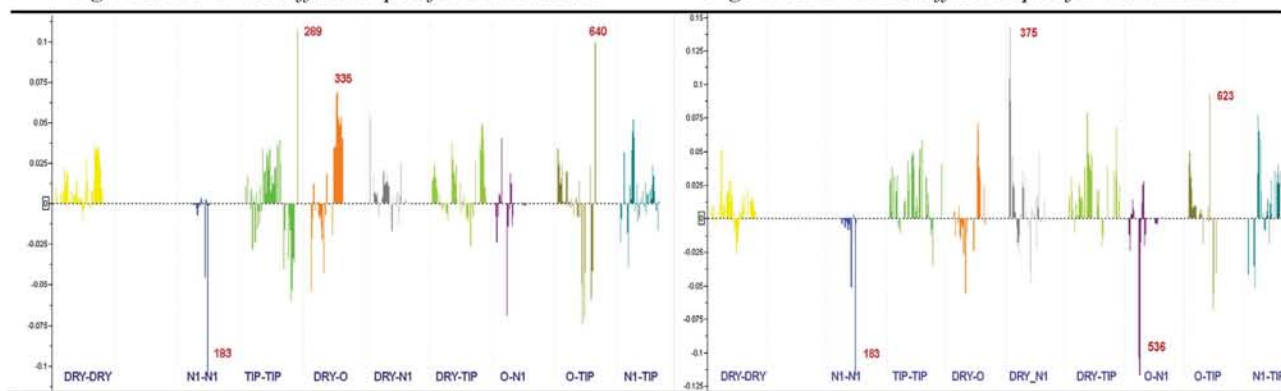


Figure 4a. FemX model,
TIP-TIP 289 (~22 Å)

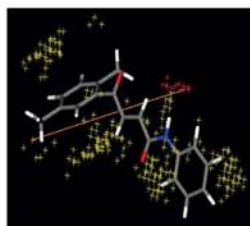


Figure 4b. FemX model,
DRY-O 336 (~13 Å).

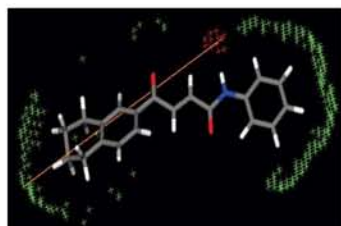


Figure 4c. FemX model,
O-TIP 640 (~16 Å)

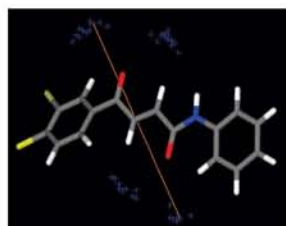


Figure 4d. FemX model,
NI-NI 183 (~12 Å)

Similarity search on compounds included in National Cancer Institute – Developmental Therapeutics Program (NCI-DTP) mechanistic database, and using **3** and **8** as templates (as described in ‘methods’), revealed similar compounds, that shares common spatial arrangement of pharmacophoric points. Five most similar compounds are: Hycantone (CAS 23255938, alkylating agent, av. GI₅₀ ~10 μM), Brequinar (CAS 96201886, RNA/DNA antimetabolite av. GI₅₀ 1.17 μM), Dichloroallyl lawsone (CAS 36417160, RNA/DNA antimetabolite av. GI₅₀ 6.98 μM), Colchicine (CAS 64-86-8, tubulin cytoskeleton destabilization, av. GI₅₀ 5 nM), 7-Chlorocampotecin (CAS 41646-05-3, Topoisomerase I inhibitor, av. GI₅₀ 45.6 nM).

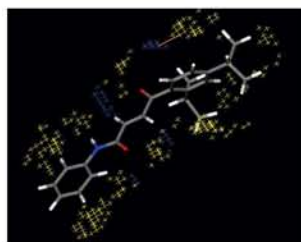


Figure 5a. HeLa model,
DRY-NI 375 (1.6-1.9 Å)

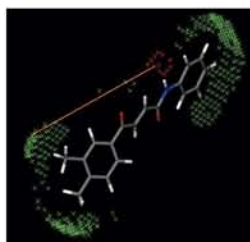


Figure 5b. HeLa model,
NI-TIP 623 (9.9-10.2 Å)

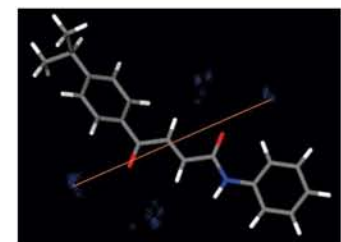


Figure 5c. HeLa model, NI-NI
183 (~11.5 Å)

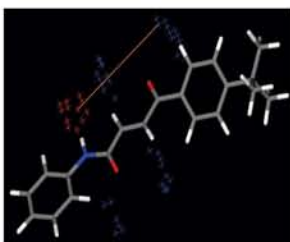


Figure 5d. HeLa model,
O-N1 536 (~6 Å)

substituent of **6**. This emphasize importance of introduction of branched alkyl substituents on aryl phenyl ring in position different of **4**; we have similar situation for parent **V**, and derivatives.²² Similar as for FemX variable N1-N1 183, which describe interaction of HBD with both oxo functionalities of molecules is negatively correlated with potency and absent for most potent **8** and **6**, as well as for **2** and **4**. Again, spatial arrangement between aryl phenyl ring and aryl keto group play important role.

Acknowledgement: Ministry of Science of Serbia support this work, grant 142010. BJD gratefully acknowledge Manuel Pastor, GRIB-CADD Universitat Pompeu Fabra, Spain and MolecularDiscovery Ltd., UK for Pentacle prerelease; as well as OpenEye Scientific Software for OMEGA, Jimmy Stewart for MOPAC2009 and Alessandro Pedretti, Istituto di Chimica Farmaceutica e Tossicologica "Pietro Pratesi" Facolta di Farmacia, Universita degli Studi di Milano, Milan, Italy for VegaZZ licenses.

Фениламиди (E)-4-арил-4-оксо-2-бутенских киселина.
Дизајн, антипсолиферативна активност, 3Д квантитативна студија структуре и
активност заснована на алгоритму АМАНДА и сличност са једињењима из
'механистичког сета' Националног института за рак САД

Синтетизовано је и потпуно окарактерисано 13 фениламида (E)-4-арил-4-оксо-2-бутенских киселина. Сва једињења показују антипсолиферативну активност према ћелијама хуманог тумора грила материце (HeLa) и хуманог меланома (FemX) у ниским микромоларним и субмикромоларним концентрацијама. Тродимензионална анализа структуре и активности је показала да међусобни распоред алкил супституената на ароил прстену, њихов просторни положај према даваоцима и примаоцима водоничне везе у молекулу, као и енергије интеракције са употребљеним пробама утичу на активност једињења за обе испитиване ћелијске линије. Два једињења (структурно довољно различита) која показују висок степен активности према обе испитиване ћелијске линије су упоређена са механистичким сетом националног института за рак САД. У оквиру тог сета и применjenог метода, како је описано у саопштењу, пет једињења која су алатијући агенси и антиметаболити РНК/ДНК показују највећу сличност по распореду фармакофорних тачака са једињењима коришћеним за поређење.

References:

1. Kumar, S. K.; Hager, E.; Pettit, C.; Gurulingappa, H.; Davidson, N. E.; Khan, S. R. *J. Med. Chem.* **2003**, *46*, 2813.
2. Cabrera, M.; Simoens, M.; Falchi, G.; Lavaggi, M. L.; Piro, O. E.; Castellano, E. E.; Vidal, A. L.; Azqueta, A.; Monge, A.; Lopez de Cerain, A.; Sagrera, G.; Seoane, G.; Cerecetto, H.; Gonzalez, M. *Bioorg. Med. Chem.* **2007**, *15*, 3356.
3. Nakamura, C.; Kawasaki, N.; Miyataka, H.; Jayachandran, E.; Kim, I. H.; Kirk, K. L.; Taguchi, T.; Takeuchi, Y.; Horie, H.; Satoha, T. *Bioorg. Med. Chem.* **2002**, *10*, 699.
4. Modzelewska, A.; Pettit, C.; Achanta, G.; Davidson, N. E.; Huang, P.; Khan, S. R. *Bioorg. Med. Chem.* **2006**, *14*, 3491.
5. Liu, X.; Go, M. *Bioorg. Med. Chem.* **2006**, *14*, 153.
6. Dimmock, J. R.; Jha, A.; Zello, G. A.; Allen, T. M.; Santos, C. L.; Balzarini, J.; De Clercq, E.; Manavathu, E. K.; Stables, J. P. *Pharmazie*, **2003**, *58*, 227.
7. Robinson, T-P.; Hubbard, R. B.; Ehlers, T. J.; Arbiser, J. L.; Goldsmith, D. J.; Bowen, J. P. *Bioorg. Med. Chem.* **2005**, *13*, 4007.
8. Yellaturu, C. R.; Manjula, B.; Neeli, I.; Rao, G. N. *J. Biol. Chem.* **2002**, *227*, 40148.
9. Jensen, L. H.; Renodon-Corniere, A.; Wessel, I.; Langer, S. W.; Søkilde, B.; Carstensen, E. V.; Sehested, M.; Jensen, P. B. *Mol. Pharmacol.* **2002**, *61*, 1235.
10. Jha, A.; Mukherjee, C.; Rolle, A. J.; De Clercq, E.; Balzarini, J.; Stables, J. P. *Bioorg. Med. Chem. Lett.* **2007**, *17*, 4545
11. a) Juranić, Z.; Stevović, L.J.; Drakulić, B.; Stanojković, T.; Radulović, S.; Juranić, I. *J. Serb. Chem. Soc.* **1999**, *64*, 505. b) Drakulić, B. J.; Stanojković, T. P.; Žižak, Ž. P. unpublished results.
12. Kulsa, P.; Hoff, D. R.; Mrozik, H. H. **1977**, US Pat. 4130661, Merck & Co., Inc. Rahway, N.J.
13. a) Mosmann, T.; *J. Immunol. Methods* **1983**, *65*, 55. b) Ohno, M.; Abe, T. *J. Immunol. Methods* **1991**, *145*, 199.
14. a) Boström, J. *J. Computer-Aided Mol. Des.* **2002**, *15*, 1137. b) Boström, J.; Greenwood, J. R.; Gottfries, J. *J. Mol. Graph. Mod.* **2003**, *21*, 449. www.eyesopen.com
15. Halgren, T. A. *J. Compu. Chem.* **1999**, *720*.
16. Stewart, J. J. P. *J. Mol. Mod.* **2007**, *13*, 1173.
17. MOPAC2009, Stewart, J. J. P., Stewart Computational Chemistry, Colorado Springs, CO, USA, **2009**, <http://OpenMOPAC.net>
18. VegaZZ 2.0.3; Pedretti, A.; Villa, L.; Vistoli, G. *J. Computer-Aided Mol. Des.* **2004**, *18*, 167. <http://www.ddl.unimi.it/>
19. Pentacle 1.0.3; Durán, Á.; Martínez, G. C.; Pastor, M. *J. Chem. Inf. Model.* **2008**, *48*, 1813. <http://cadd.imim.es/grib-cadd/projects/pentacle>, <http://www.moldiscovery.com>
20. GRID22b; Goodford, P. *J. J. Med. Chem.* **1985**, *28*, 849 (1985). <http://www.moldiscovery.com>
21. a) Weinstein, J. N.; Kohn, K. W.; Grever, M. R.; Viswanadhan, V. N.; Rubinstein, L. V.; Monks, A. P.; Scudiero, D. A.; Welch, L.; Koutsoukos, A. D.; Chiausa, A. J.; Paull, K. D. *Science* **1992**, *258* (5081), 447. b) van Osdol, W. W.; Myers, T. G.; Paull, K. D.; Kohn, K. W.; Weinstein, J. N. *J. Natl. Cancer Inst.* **1994**, *86* (24), 1853.
22. Drakulić, B. J.; Juranić, Z. D.; Stanojković, T. P.; Juranić, I. O. *J. Med. Chem.* **2005**, *48*, 5600.